

## DYNAMIC FAILURE OF STRUCTURES WITH STRUCTURAL INSTABILITY

*By Akinori NAKAJIMA\*, Shigeru KURANISHI\*\* and Hidehiko ABE\*\*\**

The objective of this paper is to discuss analytically the mechanism of dynamic failure of SDOF systems with structural instability. Furthermore, the effects of natural frequency, static load, viscous damping, and magnitude and type of dynamic load on the displacement response and the various energy quantities are also numerically investigated.

As a result, it is revealed that the effective input energy is the most important response parameter which determines the dynamic ultimate state.

*Keywords: dynamic failure, structural instability, effective input energy.*

### 1. INTRODUCTION

Failures of structures under dynamic loads are roughly classified into two types according to whether it is accompanied by the structural instability or not. The former is the case where structures subjected to static and dynamic loads come up to collapse due to development of the overall or local structural instability and yielding of material. The latter is the case where the stress of material reaches the ultimate strength such as tensile strength, or fatigue failure occurs. The failure of structures characterized by dynamic unstable behavior is considered to be either of those two types. In order to obtain the dynamic failure criteria of a structure under dynamic load, the type of failure should be first clarified and its dynamic characteristics must be investigated.

However, further accumulation of results of researches is required to establish the dynamic failure criteria. This paper deals with the type of dynamic failure of structures with structural instability, such as columns under axial compression. The structure with structural instability is the one subjected to a static load which causes an unstable behavior such as buckling, but is smaller than the critical load.

Recently, a number of studies based on the concept of limit state design have been carried out to investigate the dynamic ultimate strength or to establish the dynamic failure criteria of structures. Housner is one of the pioneers who investigated this problem<sup>1,2)</sup>. He tried to design several aseismic structures on the basis of the energy concept. A further progress in these researches was accomplished by Kato and Akiyama<sup>3,4)</sup>.

\* Member of JSCE, Dr. of Engrg., Research Associate, Dept. of Civil Engrg., University of Utsunomiya (Utsunomiya 321 Japan)

\*\* Member of JSCE, Dr. of Engrg., Professor, Dept. of Civil Engrg., Tohoku University (Sendai 980 Japan)

\*\*\* Member of JSCE, Dr. of Engrg., Professor, Dept. of Civil Engrg., University of Utsunomiya

Subsequently, a number of studies have been carried out to evaluate the earthquake resistance of structures subjected to the earthquake excitation by comparing the energy absorbed by the inelastic deformation with the input energy<sup>(5)~(10)</sup>. In these studies, however, the relation between the energy absorption in a structure and the dynamic failure of the structure seems uncertain. Most of these studies also deal with a shear vibrating system, but analysis of a flexural vibrating system is required to investigate the dynamic failure of a structure with structural instability.

The dynamic behaviors of structures with structural instability were investigated by the writers<sup>(11)~(13)</sup>. These researches indicate that the dynamic failure of columns and arch bridges subjected to periodic disturbing forces is affected by the combination of the structural instability and the yielding of materials. Ishida and Morisako discussed the dynamic failure of a single-degree-of-freedom system with gravity effect<sup>(14)</sup>. However, the relationships between this type of dynamic failure and the response parameters of structures is not sufficiently known.

The objective of this paper is to discuss analytically the mechanism of dynamic failure of a single-degree-of-freedom system with structural instability. Furthermore, the effects of natural frequency, static load, viscous damping, and magnitude and type of dynamic load on the displacement response and various energy quantities which determine the dynamic failure state are numerically investigated.

2. ELASTO-PLASTIC RESPONSE OF SDOF SYSTEM WITH STRUCTURAL INSTABILITY

(1) Equation of motion

A horizontal motion of a single-degree-of-freedom system, consisting of a mass, a rigid bar and a rotational spring as shown in Fig. 1 is considered here. The flexural vibrating system is subjected to a static load  $P$ . In this figure,  $m$  is the mass,  $k$  is the rotational spring constant,  $l$  is the length of the rigid bar,  $\theta$  is the rotational angle of the bar and  $f(t)$  is the horizontal disturbing force. If a viscous damping is not taken into account, the equation of motion for the system is as follows :

$lm\ddot{x} + R(\theta) - Px = lf(t)$ ..... (1)

in which  $R(\theta)$  is the restoring moment of the spring and within the elastic range,  $R(\theta)$  is expressed as  $k\theta$ . Furthermore, in Eq. (1), the angle of rotation of the spring is assumed to be so small that the geometrical nonlinearity is not taken into account. Therefore, substituting an approximate relationship  $\theta = x/l$  into Eq. (1), the following equation is obtained :

$m\ddot{x} + k(1-\alpha)x/l^2 = f(t)$ ..... (2)

in which the static load  $P$  is defined by

$P = \alpha k/l$ ..... (3)

In this expression, if  $\alpha=1$ , the static load becomes the critical one, so  $\alpha$  represents the ratio of the

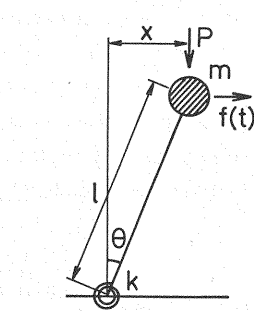


Fig.1 SDOF system with structural instability.

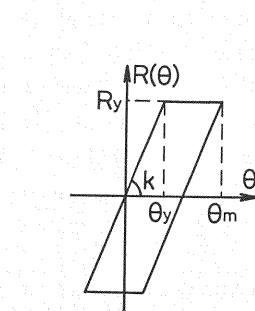


Fig.2 Restoring characteristics of rotational spring.

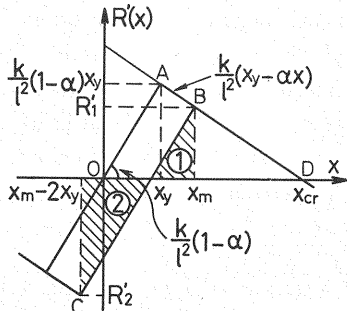


Fig.3 Restoring characteristics of system.

applied static load to the critical load (the static load ratio). According to Eq. (2), the stiffness of the system becomes smaller and then the natural frequency decreases with increasing  $\alpha$  in the range  $0 < \alpha < 1$ .

## (2) Elasto-plastic response

If the restoring characteristics of the rotational spring of the system shown in Fig. 1 is ideal elasto-plastic as shown in Fig. 2 and the spring yields in the positive direction, the restoring moment of the spring  $R(\theta)$  for the unloading path becomes

$$R(\theta) = R_y - k(\theta_m - \theta) \quad (4)$$

in which  $R_y$  is the yield restoring moment and  $\theta_m$  is the angle of rotation of the spring at the point where unloading occurs in the plastic range. In this analysis, the effect of local buckling behavior on the above restoring characteristics is not taken into account. Substituting Eq. (4) into Eq. (1), the equation of motion is

$$m\ddot{x} + (k/l^2)[x_y - x_m + (1-\alpha)x] = f(t) \quad (5)$$

The second term of this equation represents the restoring force of the system for the unloading path and Fig. 3 shows its characteristics. In this figure,  $x_y$  is the yield displacement and  $x_m$  is the plastic displacement of the mass corresponding to  $\theta_m$ , and they have the following relationships:

$$x_y = l\theta_y \quad \text{and} \quad x_m = l\theta_m \quad (6)$$

Referring to Fig. 3, it is noted that the restoring force decreases gradually as the displacement increases beyond the yield displacement. For the elastic unloading path BC, the restoring force  $R'_1$  at the point B, where the displacement  $x = x_m$ , is

$$R'_1 = (k/l^2)[(1-\alpha)x_y - \alpha(x_m - x_y)] \quad (7)$$

On the other hand, the restoring force  $R'_2$  at the point C, where the rotational spring yields in the opposite direction, is

$$R'_2 = -(k/l^2)[(1-\alpha)x_y + \alpha(x_m - x_y)] \quad (8)$$

From Eqs. (7) and (8), the following inequality is given:

$$|R'_2| > |R'_1| \quad (9)$$

This expresses that for the elastic path BC in Fig. 3, the negative yield restoring force is greater than the positive one. Thus, the elastic strain energy represented by the hatched area ② is also greater than the one represented by the hatched area ① as shown in Fig. 3. The difference of the strain energy  $E_d$  between ① and ② becomes

$$E_d = 2(k/l^2)\alpha(x_m - x_y)x_y = 4\alpha(x_m - x_y)E_y/x_y \quad (10)$$

in which  $E_y$  is the elastic strain energy up to the yielding of the spring ( $k\theta_y^2/2$ ). Thus, if the input energy exerted by the disturbing force per a half cycle is constant, the fact that the elastic strain energy ② is greater than ① as shown in Fig. 3 indicates that the mass of the system easily moves to the direction where the spring has yielded. According to Eq. (10),  $E_d$  increases as the plastic displacement  $x_m$  and/or the static load ratio  $\alpha$  increase.

Here, the case where the response of the system subjected to the following harmonic disturbing force is considered:

$$f(t) = -mZ\sin\omega t \quad (11)$$

in which  $Z$  is the acceleration amplitude and  $\omega$  is assumed as equal to the natural circular frequency as follows:

$$\omega^2 = (k/l^2)(1-\alpha)/m \quad (12)$$

If the displacement of the mass is assumed as the following stationary form:

$$x = x_m \cos\omega t \quad (13)$$

then, the velocity response is

$$\dot{x} = -\omega x_m \sin\omega t \quad (14)$$

In this condition, the input energy  $E_w$  exerted by the disturbing force in a half cycle is written as



The system shown in Fig. 1 has the maximum elasto-plastic energy absorption  $E_{su}$ . Then, as mentioned above, the system will reach the collapse state, when the input energy  $E_f$  becomes greater than  $E_{su}$ , if the hysteretic energy  $E_h$  and the kinetic energy  $E_k$  is not taken into account.

In a transient state that the displacement of the mass remains smaller than the critical displacement as shown in Fig. 4, the velocity of the mass is not always zero, that is, the system has a corresponding kinetic energy  $E_k$ . If  $E_k$  is greater than the hatched area  $E_{sr}$  in Fig. 4 (hereafter called the residual strain energy), the displacement of the mass reaches the critical one and the system collapses dynamically without any subsequent input energy. This implies that the substantial dynamic ultimate state comes before the displacement of the mass reaches the critical one. Considering the amount of energy up to the dynamic ultimate state according to Eq. (20) and Fig. 4, the system will collapse, if the sum of  $E_s$  and  $E_k$ , that is, the effective input energy  $E_{ef}$ , which is obtained by subtracting the hysteretic energy  $E_h$  from the input energy  $E_f$ , is greater than  $E_{su}$ . Therefore, the transient state in which the effective input energy  $E_{ef}$  exceeds  $E_{su}$  first is defined as the dynamic ultimate state and the displacement in this state is defined as the dynamic ultimate displacement  $x_u$ . The above mentioned relationship is expressed as follows :

$$E_{su} = E_s + E_{sr} \leq E_s + E_k = E_f - E_h = E_{ef} \quad (23)$$

For the system with viscous damping, the energy dissipated by the damping should be considered in Eq. (23).

### 3. RESULTS OF NUMERICAL ANALYSIS

#### (1) Elasto-plastic response by numerical method and definition of dynamic ultimate state

It is so difficult to obtain analytically the responses in the dynamic ultimate state defined in the previous section, that it is better to obtain the responses of the system shown in Fig. 1 by a numerical method. A step by step integration, where the modified Newton-Raphson method and the Newmark  $\beta$  method ( $\beta = 1/4$ ) are combined, is employed<sup>(1)</sup>. The restoring characteristics of the rotational spring are also assumed to be ideal elasto-plastic. For the Newmark  $\beta$  method, the time interval which is equal to  $1/128$  of the natural period of the system is chosen.

Here, the natural frequency, the static load, the viscous damping, the yield displacement and the type and magnitude of the periodic disturbing force are considered to be taken as parameters. Hereafter, unless otherwise mentioned, the responses of the system with a constant yield displacement and no viscous damping are investigated, when the system is subjected to a harmonic disturbing force at resonance. Then the main purpose of the numerical analysis is to investigate the effects of the natural frequency, the static load and the amplitude of the harmonic disturbing force on the dynamic ultimate state. The static load refers to the one normalized by the critical load (the static load ratio  $\alpha$ ) and the amplitude of the disturbing force refers to the one normalized by the yield restoring force (the yield strength coefficient  $\gamma$ ). For example, considering the main compression members of truss bridge, the value of  $\alpha$  is taken as 0.5, and other two variations 0.25 and 0.75 are added for examination of the effect of  $\alpha$ . Furthermore, since the natural frequency varies with the magnitude of the static load as given by Eq. (12), the natural frequency refers to the one without the effect of the static load.

The displacement-time curve  $C_0$  is shown in Fig. 5, when the natural frequency  $n=5\text{Hz}$ , the static load ratio  $\alpha=0.5$  and the yield strength coefficient  $\gamma=50$ . The abscissa shows the time normalized by the natural period of the system  $T$  and the ordinate shows the displacement normalized by the yield displacement. The rotational spring yields due to the increase of the vibrational amplitude at resonance, and the equilibrium position of the vibration shifts to one direction only. Then, the displacement increases rapidly and the system comes up to

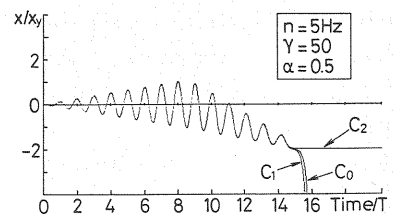


Fig. 5 Displacement-time curve under harmonic disturbing force.

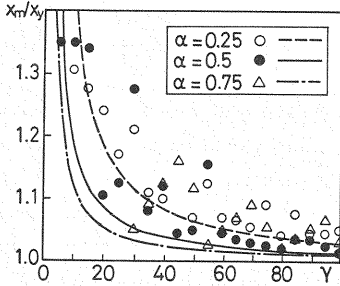


Fig. 6 Relationship between yield strength coefficient and plastic displacement, when rotational spring does not yield in opposite direction.

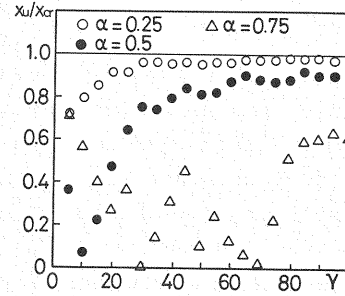


Fig. 7 Dynamic ultimate displacement under harmonic disturbing force.

collapse. Hereafter, the dynamic ultimate state is defined as the state at the initial time, after which the displacement diverges and the system collapses without subsequent application of the disturbing force. The displacement-time curve  $C_1$  shown in Fig. 5 corresponds to the case where the displacement diverges in the system subjected to no disturbing force after a specified time  $t_i$ . On the other hand, the displacement-time curve  $C_2$  corresponds to the case where the displacement does not diverge in the system subjected to no disturbing force after the time  $t_{i-1}$ . Therefore, the system comes up to the dynamic ultimate state at the specified time  $t_i$ . This state is consistent with the one described in the previous section.

It is noted that the displacement shifts gradually to one direction, because the stiffness of the system has a negative value, such as the path AB shown in Fig. 3, due to yielding of the rotational spring. That is, the yield restoring force decreases in the yielding direction and increases in the opposite direction, as discussed previously in Sec. 2. (2). In this case, whether yielding occurs or not in the opposite direction depends on the amplitude of the disturbing force. Fig. 6 shows the relationship between the yield strength coefficient  $\gamma$  and the plastic displacement  $x_m$ , when in the numerical analysis the rotational spring does not yield consecutively in the opposite direction. The ordinate is the plastic displacement  $x_m$ , normalized by the yield displacement and the abscissa is the yield strength coefficient. The open circles, the closed circles and the triangles correspond to the cases of  $\alpha=0.25$ ,  $0.5$  and  $0.75$ , respectively. The dashed curve, the solid curve and the dot-dash curve are also obtained by Eq. (18), for  $\alpha=0.25$ ,  $0.5$  and  $0.75$ , respectively. Eq. (18) gives a good prediction of the plastic displacement, when the rotational spring does not yield in the opposite direction, since the most of the numerical results are scattered above the curves obtained by Eq. (18) regardless of the ratio  $\alpha$ . It can be seen numerically that if the static load ratio  $\alpha$  is constant, the plastic displacement described above depend on the amplitude of the harmonic disturbing force but not on the natural frequency, because the plot for the system with other natural frequencies is overlapped with that of Fig. 6.

## (2) Displacement response in dynamic ultimate state

The relationship between the dynamic ultimate displacement  $x_u$ , defined previously in Sec. 3. (1) and the yield strength coefficient is shown in Fig. 7. The ordinate shows the ultimate displacement normalized by the critical one and the abscissa shows the yield strength coefficient  $\gamma$ . The open circles, the closed circles and the triangles correspond to the cases of  $\alpha=0.25$ ,  $0.5$  and  $0.75$ , respectively. The ultimate displacement  $x_u$  approaches  $x_{cr}$  asymptotically as  $\gamma$  increases, in the cases of  $\alpha=0.25$  and  $0.5$ . However, for  $\alpha=0.75$ , such tendency is not remarkable, but  $x_u$  approaches  $x_{cr}$  gradually as  $\gamma$  increases in the range  $\gamma \geq 100$ . Furthermore,  $x_u$ , normalized by  $x_{cr}$ , neither depend on the natural frequency nor the yield displacement, but on the static load ratio, because the plot for the system with other natural frequencies and the yield displacement is also overlapped with that of Fig. 7.

## (3) Energy responses in dynamic ultimate state

In Fig. 8, the input energy  $E_f$  exerted by the disturbing force and the effective input energy  $E_{ef}$  which is

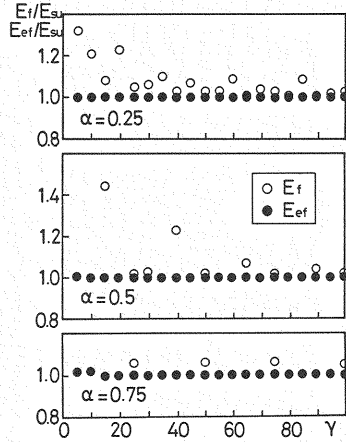


Fig. 8 Input energy under harmonic disturbing force.

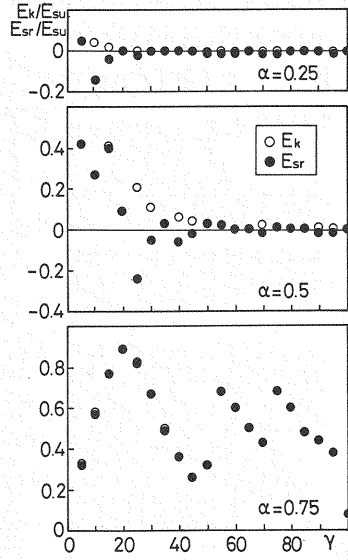


Fig. 9 Residual strain energy and kinetic energy in dynamic ultimate state.

obtained by subtracting, the energy dissipated by the hysteresis loop  $E_h$ , from the input energy are plotted against the yield strength coefficient  $\gamma$  in the dynamic ultimate state. The ordinate shows the input energy normalized by  $E_{su}$  and the abscissa shows the yield strength coefficient. The open circles express the input energy  $E_f$  and the closed circles show the effective input energy  $E_{ef}$ , for  $\alpha=0.25, 0.5$  and  $0.75$ . When  $E_f$  is equal to  $E_{ef}$ , the open circles are overlapped by the closed circles in the figure. As the difference between the input energy  $E_f$  and the effective input energy  $E_{ef}$  gets greater, the amount of energy is more dissipated by the hysteretic damping. Therefore, according to Fig. 8, the input energy may be more dissipated by the hysteretic damping as  $\alpha$  decreases, and the tendency of dissipation is more remarkable, as  $\gamma$  decreases. However, it is noted that  $E_{ef}$  is nearly equal to 1.0, irrespective of values of  $\alpha$  and  $\gamma$ . Thus, it is confirmed numerically that the system comes up to collapse, when the effective input energy  $E_{ef}$  exceeds  $E_{su}$ .

The residual strain energy  $E_{sr}$  (the hatched area shown in Fig. 4) and the kinetic energy  $E_k$ , estimated by the velocity of the mass in the ultimate state are shown against the yield strength coefficient  $\gamma$  in Fig. 9. The ordinate is the amount of energy normalized by  $E_{su}$  and the abscissa is the yield strength coefficient. The open circles and the closed circles show the kinetic energy  $E_k$  and the residual strain energy  $E_{sr}$ , respectively. In the dynamic ultimate state,  $E_k$  is nearly equal to or larger than  $E_{sr}$ , independent of values of  $\alpha$  and  $\gamma$ . This implies that the displacement of the mass without subsequent application of the disturbing

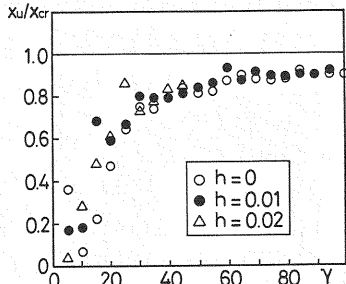


Fig. 10 Effect of viscous damping on dynamic ultimate displacement.

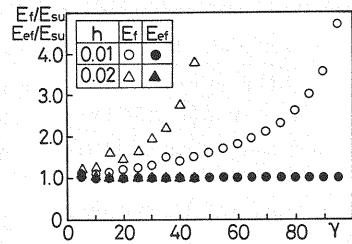


Fig. 11 Effect of viscous damping on input energy.

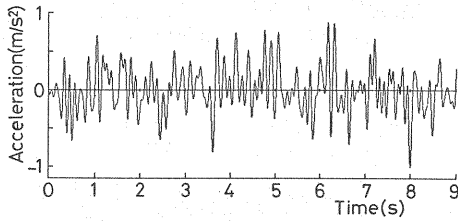


Fig. 12 Random disturbing force.

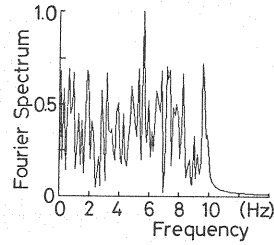


Fig. 13 Fourier spectrum of random disturbing force.

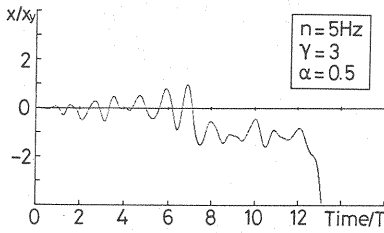


Fig. 14 Displacement-time curve under random disturbing force.

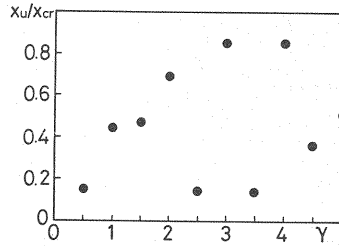


Fig. 15 Dynamic ultimate displacement under random disturbing force.

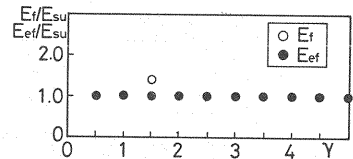


Fig. 16 Input energy under random disturbing force.

force after the dynamic ultimate state reaches the critical displacement and the system collapses. The amounts of energy  $E_{sr}$  and  $E_k$  approach zero, as  $\alpha$  decreases and  $\gamma$  increases. Furthermore, referring to Figs. 7 and 9, it can be seen that the ratio of  $x_u$  to  $x_{cr}$  becomes small, when  $E_k$  is large. In the figure, the negative value of energy means that the system comes up to the dynamic ultimate state in the position where the resoring force has a negative value and the elastic strain energy in the negative direction is greater than  $E_{sr}$  in Fig. 4. The effective input energy and the residual strain energy normalized by  $E_{su}$  are also independent of the natural frequency and the yield displacement for the same reason as the case of Fig. 7.

#### (4) Effect of viscous damping on responses in dynamic ultimate state

In the previous discussion, the effect of damping is not taken into account in the comparison of the numerical response with the analytical one. However, because the effect of damping cannot be avoided in practice, its effect on the responses in the dynamic ultimate state is investigated here. Fig. 10 shows the relationship between the yield strength coefficient  $\gamma$  and the displacement in the dynamic ultimate state  $x_u$ , when the damping constant  $h=0, 0.01$  and  $0.02$ ,  $n=5\text{Hz}$  and  $\alpha=0.5$ . The open circles, the closed circles and the triangles correspond to the cases for  $h=0, 0.01$  and  $0.02$ , respectively. The figure indicates that the value of damping constant has no influence on  $x_u$ . The cases of  $h=0.01$  with  $\gamma=100$  and  $h=0.02$  with  $\gamma \geq 50$  are not shown in the figure, because a steady-state vibration occurs before the rotational spring yields.

The input energy  $E_f$  and the effective input energy  $E_{ef}$  up to the dynamic ultimate state are shown against the yield strength coefficient  $\gamma$  in Fig. 11, when  $h=0.01$  and  $0.02$ . From this figure and Fig. 8, where the viscous damping is not considered, it is clear that the input energy  $E_f$  increases as the damping constant increases. In particular, this tendency is remarkable for large values of  $\gamma$ . However, the effective input energy  $E_{ef}$  is little affected by the damping, and is nearly equal to  $E_{su}$ .

#### (5) Behavior of dynamic failure under random disturbing force

The behavior of the system at the dynamic failure under a harmonic disturbing force is investigated fundamentally in the preceding sections. Now the case where the system is subjected to a random disturbing force which has the time duration of about 9 seconds and the dominant frequencies in the region of 0 to 10Hz as shown in Fig. 12 is examined. Fig. 13 shows the normalized Fourier spectrum of the disturbing force. The displacement-time curve of the system is shown in Fig. 14 in the cases of  $n=5\text{Hz}$ ,  $\alpha=0.5$  and  $\gamma=3.0$ .

After yielding, the displacement shifts to one direction only and grows rapidly. This behavior is similar to that under the harmonic disturbing force shown in Fig. 5, and the behavior at the dynamic failure is not affected by the type of the disturbing force.

Fig. 15 shows the relationship between the yield strength coefficient  $\gamma$  and the displacement  $x_u$  of the system subjected to the random disturbing force in the dynamic ultimate state. The displacement  $x_u$  tends to approach the critical displacement  $x_{cr}$ , but the tendency is not so remarkable as the case where the system is subjected to the harmonic disturbing force. Furthermore, the input energy  $E_f$  and the effective input energy  $E_{ef}$  up to the dynamic ultimate state are shown in Fig. 16 in relation to the yield strength coefficient  $\gamma$ .  $E_f$  is nearly equal to  $E_{ef}$ , because the yielding occurs in one direction only and the restoring curves does not form a hysteretic loop, and consequently the input energy is not dissipated by the hysteretic damping, and the effective input energy agrees with  $E_{su}$ .

From the results of numerical analysis, it can be said conclusively that the effective input energy may be the most important response parameter which affects the dynamic ultimate state of a vibrating system with structural instability. This energy is obtained by subtracting the energy dissipated by the hysteretic damping and the damping from the input energy exerted by the disturbing force, and coincides with the maximum elasto-plastic energy absorbed up to the critical state.

## 5. CONCLUSIONS

In order to study the behavior at the dynamic failure of a structure with structural instability, the dynamic failure of a single-degree-of-freedom system subjected to static and dynamic loads is analytically and numerically examined. The effects of natural frequency, static load, yield displacement, viscous damping, and type and magnitude of disturbing force on the behavior at the dynamic failure are investigated, and the following findings are obtained ;

(1) The dynamic failure of a system with structural instability is characterized by the following behaviors. That is, after yielding of the rotational spring, the equilibrium position of the vibration shifts to one direction only and the displacement of the mass grows infinitely. The shift of the vibration occurs, because the yield restoring force of the system in the yielding direction decreases and the one in the opposite direction increases after yielding. Furthermore, the dynamic failure due to infinite development of the displacement response takes place, because the elasto-plastic strain energy absorption excluding the hysteretic energy has the maximum value and the excessive input energy causes further deformation, which results in further decrease of the strain energy absorption.

(2) The substantial dynamic ultimate state comes before the displacement of the mass reaches the critical one, in which the elasto-plastic strain energy has a maximum value. The displacement in the dynamic ultimate state is smaller than the critical one and asymptotically approaches the critical displacement as the amplitude of the disturbing force decreases.

(3) In the dynamic ultimate state, the kinetic energy is greater than the residual strain energy which will be absorbed in the system from the dynamic ultimate state to the critical state. Therefore, the displacement reaches the critical one and the system comes up to collapse.

(4) The effective input energy may be the most important response parameter which determines the dynamic ultimate state. This energy is obtained by subtracting the energy dissipated by the hysteretic damping and the damping from the input energy exerted by the disturbing force. When the effective input energy exceeds the maximum elasto-plastic energy absorption, the system comes up to collapse. It is not affected by the natural frequency, the normalized magnitude of the static load, damping, the yield displacement nor the type and normalized magnitude of the disturbing force.

## ACKNOWLEDGEMENT

This study was supported in part by the Grand-in-Aid for Encouragement of Young Scientist from the

Japanese Ministry of Education, Science and Culture.

#### REFERENCES

- 1) Housner, G.W. : Limit design of structures to resist earthquakes, Proc. of 1st WCEE, 1956.
- 2) Housner, G.W. : Behavior of structures during earthquakes, Proc. of ASCE, Vol.85, EM 4, pp.109~129, October, 1959.
- 3) Kato, B. and Akiyama, H. : Energy input and damages in structures subjected to severe earthquakes, Transaction of A. I. J., No.235, pp.9~18, September, 1975 (in Japanese).
- 4) Akiyama, H. : Earthquake-Resistant Limit-State Design for Building, University of Tokyo Press, Tokyo, 1985.
- 5) Ohno, T., Nishioka, T. and Fujino, Y. : Quantitative estimation of plastic energy absorbed in structures subjected to seismic excitation, Proc. of JSCE, No.333, pp.91~99, May, 1983 (in Japanese).
- 6) Yamada, Y., Iemura, H., Furukawa, K. and Sakamoto, K. : An optimum aseismic design of inelastic structures with target ductility requirements, Proc. of JSCE, No.341, pp.87~95, January, 1984 (in Japanese).
- 7) Hakuno, M. and Morikawa, O. : A simulation on important factors to collapse of structures due to earthquake, Proc. of JSCE, No.344/I-1, pp.299~302, April, 1984 (in Japanese).
- 8) Zahrah, T.F. and Hall, W.J. : Earthquake energy absorption in SDOF structures, Proc. of ASCE, Vol.110, No.ST 8, pp.1757~1772, August, 1984.
- 9) Ohno, T. and Nishioka, T. : Control of input energy for elastic-plastic multi-mass systems subjected to seismic motion, Proc. of JSCE, Struct. Eng./Earthq. Eng., Vol.2, No.1, pp.223~233, Japan Society of Civil Engineers, April, 1985.
- 10) Hirao, K., Sawada, T., Nariyuki, Y. and Sasada, S. : On the relation between hysteretic energy and elastic responses of single degree of freedom systems under strong earthquake motions, Proc. of JSCE, No.368/I-5, pp.401~410, April, 1986 (in Japanese).
- 11) Kuranishi, S. and Nakajima, A. : Dynamic strength characteristics of axially loaded columns subjected to periodic lateral acceleration, Proc. of JSCE, No.341, pp.41~49, January, 1984.
- 12) Kuranishi, S. and Nakajima, A. : Failure of elasto-plastic columns with initial crookedness in parametric resonance, Proc. of JSCE, Struct. Eng./Earthq. Eng., Vol.2, No.1, pp.207~216, Japan Society of Civil Engineers, April, 1985.
- 13) Kuranishi, S. and Nakajima, A. : Strength characteristics of steel arch bridges subjected to longitudinal acceleration, Proc. of JSCE, Struct. Eng./Earthq. Eng., Vol.3, No.2, pp.287~295, Japan Society of Civil Engineers, October, 1986.
- 14) Ishida, S. and Morisako, K. : Collapse of SDOF system to harmonic excitation, Proc. of ASCE, Vol.111, No.EM 3, pp.431~448, May, 1985.

(Received April 20 1987)